

isotope with the 2-meter crystal spectrometer in 1949 and 1950, which formed part of his thesis for the doctorate. The first mentioned of the two sources, the narrower and the weaker of the two, was the one used by him. Actually all the wavelengths have been remeasured with the second source because certain changes in

the spectrometer in the meanwhile have rendered the applicability of our present calibration to this older data too uncertain. Nevertheless, Brown's pioneering study on this isotope has been of the greatest value to us, and it is a pleasure to acknowledge here our indebtedness to him.

PHYSICAL REVIEW

VOLUME 88, NUMBER 4

NOVEMBER 15, 1952

Penetration and Diffusion of X-Rays: Calculation of Spatial Distributions by Semi-Asymptotic Methods*

L. V. SPENCER

National Bureau of Standards, Washington, D. C.

(Received June 20, 1952)

Methods are presented for calculating x-ray spectra in an infinite homogeneous medium. These methods are particularly useful for calculating spectra at great distances from the radiation source. The transport equation is solved numerically by characterizing angular and spatial distributions with a small number of suitable parameters. Attention is called to a mathematical technique which is extremely useful for this purpose, whereby a function may be approximated from a knowledge of moments, derivatives, or values. Sample numerical applications include spectral intensities at various distances from a plane monodirectional 10.22-Mev x-ray source in Pb and a plane monodirectional 5.11-Mev source in Fe.

I. INTRODUCTION

THE very deep penetration of photons which experience multiple Compton scattering¹ has been studied previously in a number of papers.²⁻⁴ These treatments—all completely analytic—have been designed to yield information about the asymptotic form of the x-ray penetration law. In this paper we shall present a numerical approach which makes use of these asymptotic penetration laws; therefore, in Appendix A we summarize these earlier results and discuss briefly some unpublished work of the same kind.

The complicated nature of actual x-ray cross sections militates strongly against the usefulness of purely analytical methods in finding realistic spectral intensities in specific situations. Numerical methods hold much more promise. One such numerical method has been presented⁵⁻⁷ which relies on expansions in suitable spatial and directional polynomial systems. The diffusion equation is reduced through these expansions to a

form suitable for ordinary numerical integrations. This polynomial method has proved very useful for penetrations up to 16–24 mean free paths of the hardest spectral component; but it is in no sense asymptotic since the burden of the numerical integrations tends to increase rapidly with the penetration.

We present here a method for numerical calculations which might be called “semi-asymptotic.” It is capable of yielding as much information as the polynomial method, while the numerical work involved is nearly independent of the penetration. This method relies upon a Fourier-Laplace transformation in the spatial variable. In Sec. II the diffusion equation is presented and is reduced, through this spatial transformation and through integrations over photon directions, to an interlinked system of integral equations. Section III describes schematically an approach to the solution of this system. Section IV presents the method which was actually used. The success of this method is largely due to a new mathematical technique for approximating functions. In order to preserve continuity of thought, this technique is described in Appendix B rather than in the body of the text. In Sec. VII the inversion of the Fourier-Laplace transform is discussed. The details of the inversion are given in Appendix C.

The results of actual calculations for the following three problems are presented and discussed in Sec. VIII: (1) a plane monodirectional 10.22-Mev source in Pb; (2) a plane monodirectional 5.11-Mev source in Fe; (3) a plane isotropic 5.11-Mev source in Fe. Spectral intensities are given for penetrations up to 160 mean free paths in the first case and 50 mean free paths in

* Work supported by the ONR.

¹ At the low energy end of the spectrum, where the energy shift of the scattered photons can be disregarded or treated as a small correction, the diffusion of photons has been studied by S. Chandrasekhar (*Radiative Transfer*, Oxford University Press, London, 1950), but without specific reference to very deep penetrations. At the very high energy end, where large amounts of x-rays are regenerated by secondary electrons, a full development of the shower theory is required. Pair production will be treated here as a mechanism for outright absorption. (The results of this paper can be applied to the tail end of showers.)

² Bethe, Fano, and Karr, *Phys. Rev.* **76**, 538 (1949).

³ U. Fano, *Phys. Rev.* **76**, 739 (1949).

⁴ Fano, Hurwitz, and Spencer, *Phys. Rev.* **77**, 425 (1950).

⁵ L. V. Spencer and U. Fano, *Phys. Rev.* **81**, 464 (1951).

⁶ L. V. Spencer and U. Fano, *J. Research Natl. Bur. Standards* **46**, 446 (1951).

⁷ L. V. Spencer and Fannie Stinson, *Phys. Rev.* **85**, 662 (1952).

the second. The calculations for the third case are more restricted.

II. THE DIFFUSION EQUATION

We consider the penetration, degradation, and diffusion of x-rays in an infinite medium with a plane source. Under conditions of plane symmetry the spectral energy density Y of the x-rays depends only on the distance x from the source, on the obliquity ω_x of the direction of propagation ω , and on the wavelength λ (in Compton units). This energy density obeys the transport equation

$$\omega_x \partial Y(x, \omega_x, \lambda) / \partial x + \mu(\lambda) Y(x, \omega_x, \lambda) = \int_0^\lambda d\lambda' k(\lambda', \lambda) \int_{4\pi} d\omega' 1/2\pi \delta(1 - \lambda + \lambda' - \omega \cdot \omega') \times Y(x, \omega_x', \lambda') + \text{source}, \quad (1)$$

where $\mu(\lambda)$ represents the total attenuation coefficient, $k(\lambda', \lambda)$ represents the differential Klein-Nishina probability for Compton scattering of a photon of wavelength λ' into the interval from λ to $\lambda + \Delta\lambda$,^{7a} and the Dirac δ -function represents the Compton condition.

As in references 3 and 4 we represent the solution of (1) as a superposition of space distributions which decay in depth exponentially, by the method of the Fourier-Laplace transformation. The "transform" of Y , i.e.,

$$y(p, \omega_x, \lambda) = \int_{-\infty}^{\infty} dx e^{px} Y(x, \omega_x, \lambda),$$

obeys the equation

$$[\mu(\lambda) - p\omega_x] y(p, \omega_x, \lambda) = \int_0^\lambda d\lambda' k(\lambda', \lambda) \int_{4\pi} d\omega' 1/2\pi \delta(1 - \lambda + \lambda' - \omega \cdot \omega') \times y(p, \omega_x', \lambda') + \text{source}. \quad (2)$$

We are primarily interested in calculating the quantity

$$y_0(p, \lambda) = (1/2\pi) \int_{4\pi} d\omega y(p, \omega_x, \lambda).$$

The inversion of $y_0(p, \lambda)$ to obtain the depth distribution will be discussed in Sec. VII.

The "topography" of y as a function of p is as follows: y is defined on a strip parallel to the imaginary axis such that $-\mu_s \leq \text{Re} p \leq +\mu_s$, where μ_s is the attenuation coefficient of the hardest scattered x-rays. (For $|\text{Re} p| > \mu_s$, the integral defining y diverges.) The singularities of y are related to the vanishing of the factor $[\mu(\lambda) - p\omega_x]$. This occurs, within the strip of definition, only if $\mu(\lambda) \rightarrow \mu_s$, $\omega_x \rightarrow 1$. Thus, y has singularities at $\pm\mu_s$, i.e., on the real axis. (The type of singularity which y

may have at $+\mu_s$ is given in Appendix A.) Because of the location of the singularities, for every set of values (x, ω_x, λ) there must exist a saddle on the real axis for some value $|p| < \mu_s$. For large x , this saddle will be close to $+\mu_s$, while for small or negative x , the saddle will lie at small or negative values of p . Since we are primarily interested in evaluating y near the saddle point, we want to assign to p real values within the range of definition.

Clearly those components are most penetrating which have the smallest attenuation coefficient and which travel directly away from the source. The components which control the deep penetrations tend to have directional distributions strongly peaked at $\omega_x = 1$. Now, any sharply peaked distribution requires many spherical harmonics for its description. This means that spherical harmonics are not the most convenient quantities to use in describing the directional distribution of the deeply penetrating radiation.⁶ A more convenient quantity to use in characterizing these directional distributions is the "angular moment" defined as follows:

$$y_n(p, \lambda) = \frac{1}{2\pi} \int_{4\pi} d\omega (1 - \omega_x)^n y(p, \omega_x, \lambda). \quad (3)$$

In order to find equations for these angular moments, we multiply (2) by $(1 - \omega_x)^n$ and integrate over all directions. The result is the following system of equations:

$$[\mu(\lambda) - p] y_n(p, \lambda) + p y_{n+1}(p, \lambda) = \int_0^\lambda d\lambda' k(\lambda', \lambda) \sum_{n'=0}^n (\lambda - \lambda')^{n-n'} S_n^{n-n'}(\lambda - \lambda') \times y_{n'}(p, \lambda') + \text{source}, \quad (4)$$

where $S_n^{n'}(z)$ are polynomials of degree $(n - n')$,⁸

$$(-1)^{n'} [2^{n-n'} n'! (n-n')!] S_n^{n'}(z) = (d^n/dz^n) [z^{n-n'} (2-z)^n]. \quad (5)$$

Notice that the set of Eqs. (4) is interlinked by the term $y_{n+1}(p, \lambda)$ in such a way that the whole system must be solved simultaneously. Every y_n depends upon every other y_n . If $p/(\mu - p)$ is small enough, it is feasible to break the interlinkages by expanding the y_n in powers of p or perhaps $p/(\mu_s - p)$. Such a procedure is equivalent to the polynomial method.⁶ However, we are interested in solving for $y_n(p, \lambda)$ at values of p large enough so that such an expansion converges very slowly; hence we must now consider the simultaneous solution of Eqs. (4).

III. DISCUSSION

In order to solve Eqs. (4) simultaneously, we may resort to trial and error methods. We may define a

⁸ These (Jacobi type) polynomials are self-adjoint over the interval $0 \leq z \leq 2$ with respect to the weight function z^n .

^{7a} Since Y refers to energy density rather than number density, the function $k(\lambda', \lambda)$ referred to here differs from that in reference 6 by a factor (λ/λ') .

function $g_1(p, \lambda) = y_1(p, \lambda)/y_0(p, \lambda)$. If we guess this function, the whole chain of equations can be unraveled and values for all the y_n 's can be obtained. However, these values for the angular moments will correspond to a well-behaved function⁹ only if $g_1(p, \lambda)$ has been guessed correctly. Thus $g_1(p, \lambda)$ plays the role of an "eigenvalue."¹⁰ This suggests that if it is possible to determine whether or not a set of values for the $y_n(p, \lambda)$ correspond to the moments of a well-behaved function, it may be possible to determine whether or not any estimated $g_1(p, \lambda)$ is correct.

Because Compton scattering always increases the photon wavelength λ , the integration of (4) proceeds naturally from smaller to larger λ 's. As a matter of fact, if $y(p, \omega_x, \lambda')$ is known for all $\lambda' < \lambda$, then $y(p, \omega_x, \lambda)$ must be completely determined. Thus, if a numerical integration could be made of the whole infinity of Eqs. (4) simultaneously, using infinitely small integration steps, it would yield automatically the correct solution; and no "eigenvalue problem" would exist. Such an idealized procedure can be outlined in the angular moment scheme as follows: If the infinity of quantities $y_n(p, \lambda')$, $\lambda' < \lambda$, are known, the right-hand sides of Eqs. (4) are completely determined except for a single infinitesimal interval which can be neglected. Furthermore, according to (2) the right sides of Eqs. (4) are the angular moments of the quantity $R(p, \omega_x, \lambda) = [\mu(\lambda) - p\omega_x]y(p, \omega_x, \lambda)$. Because we know an infinity of these moments, we can determine $R(p, \omega_x, \lambda)$ and thereby $y(p, \omega_x, \lambda)$ exactly.

In practice such a perfect integration scheme is impossible, of course. It is necessary to use finite steps of integration and a finite number of equations. This means that incomplete information about $y(p, \omega_x, \lambda')$, for $\lambda' < \lambda$, must suffice in our determination of $y(p, \omega_x, \lambda)$. The problem is thus to find a procedure for making such "educated estimates" of $g_1(p, \lambda)$ that no harm arises from the lack of complete information about $y(p, \omega_x, \lambda')$ for $\lambda' < \lambda$.

The critical information which apparently must be included in any such procedure is the fact that $y(p, \omega_x, \lambda)$ and therefore $R(p, \omega_x, \lambda)$ are well-behaved functions of ω_x . Thus, our method of solution (which is outlined in greater detail in the next section) is to determine at each step of a progressive numerical integration in λ , an approximate function $\bar{R}(p, \omega_x, \lambda)$. This function has three properties:

- (a) The first r angular moments of \bar{R} agree with the right sides of the first r Eqs. (4).
- (b) \bar{R} is well-behaved.

⁹ By "well-behaved function" we mean a function which is positive and finite (except possibly for known δ -function terms) and agrees with as much of our other *a priori* information, such as number and location of maxima and discontinuities, as it is feasible to consider.

¹⁰ Other combinations of the y_n 's can be used as well in this connection. The function $g_1(p, \lambda)$ is chosen here because of other advantages discussed in Sec. VI.

(c) The first r approximate angular moments $\bar{y}_n(p, \lambda)$ which occur on both sides of (4), are given by the relations

$$\bar{y}_n(p, \lambda) = \int_{-1}^1 d\omega_x (1 - \omega_x)^n \frac{\bar{R}(p, \omega_x, \lambda)}{\mu(\lambda) - p\omega_x}. \quad (6)$$

These approximate values, $\bar{y}_n(p, \lambda)$, then enter into the integrals in (4) for all further integrations.

The accuracy of this method depends upon the integration technique and also upon how well we can describe R with r angular moments. Section V is a discussion of this point.

IV. AN ITERATION PROCEDURE

Having decided to use numerical procedures to integrate Eqs. (4), we now write the integrals as sums:

$$\begin{aligned} & [\mu(\lambda_l) - p]\bar{y}_n(p, \lambda_l) + p\bar{y}_{n+1}(p, \lambda_l) \\ &= \sum_{i=0}^l \Delta\lambda_i a_i k(\lambda_i, \lambda_l) \sum_{n'=0}^n (\lambda_l - \lambda_i)^{n-n'} \\ & \quad \times S_n^{n-n'} (\lambda_l - \lambda_i) \bar{y}_{n'}(p, \lambda_i) + \text{source}. \end{aligned} \quad (7)$$

The a_i are the weights associated with some integration formula or combination of integration formulas. The $\Delta\lambda_i$ need not be all the same size. The bar over the various quantities indicates that we are working now with approximate quantities limited in accuracy by the finiteness of the integration intervals and by the number of moment equations used. If we separate the l th term from the sum on the right, we have

$$\begin{aligned} & [\mu(\lambda_l) - p]\bar{y}_n(p, \lambda_l) + p\bar{y}_{n+1}(p, \lambda_l) \\ &= [\Delta_l a_l k(\lambda_l, \lambda_l) \bar{y}_n(p, \lambda_l)] \\ & \quad + \sum_{i=0}^{l-1} \Delta\lambda_i a_i k(\lambda_i, \lambda_l) \sum_{n'=0}^n (\lambda_l - \lambda_i)^{n-n'} \\ & \quad \times S_n^{n-n'} (\lambda_l - \lambda_i) \bar{y}_{n'}(p, \lambda_i) + \text{source}. \end{aligned} \quad (8)$$

Consider a situation in which we have determined $\bar{y}_n(p, \lambda_i)$ for $0 \leq \lambda_i \leq \lambda_{l-1}$. We are now in a position to calculate the right hand side of Eqs. (8) except for the term in brackets. This term can be made small relative to the other terms on the right by taking $\Delta\lambda_l$ sufficiently small. Furthermore, since the y_n 's must be continuous functions a good estimate can be made of this term. We now perform the following sequence of operations:

(a) We estimate the $\bar{y}_n(p, \lambda_l)$ and call our estimate $\bar{y}_n^0(p, \lambda_l)$.

(b) We insert the $\bar{y}_n^0(p, \lambda_l)$ into the bracketed terms of (8) and thus calculate the right sides of (8). We call these quantities $\bar{R}_n^0(p, \lambda_l)$. These $\bar{R}_n^0(p, \lambda_l)$ are the zero'th approximation to the moments of

$$\bar{R}(p, \omega_x, \lambda_l) = [\mu(\lambda_l) - p\omega_x] \bar{y}(p, \omega_x, \lambda_l).$$

(c) We construct a well-behaved function $\bar{R}^0(p, \omega_x, \lambda_l)$, whose first moments are the quantities $\bar{R}_n^0(p, \lambda_l)$. This is our main problem. Methods for doing it are discussed later in this section and in Appendix B. In problems involving a plane, monodirectional source, where r equations are used, we have taken

$$\bar{R}^0(p, \omega_x, \lambda_l) = \sum_{m=1}^{r/2} \frac{\eta_m}{\beta_m} e^{-(1-\omega_x)/\beta_m} + D(p, \omega_x, \lambda_l), \quad (9)$$

where $D(p, \omega_x, \lambda_l)$ represents essentially the effect of low orders of scattering, which we can calculate exactly. The r parameters, η_m and β_m , are so chosen that the first r moments of $\bar{R}^0(p, \omega_x, \lambda_l)$ are equal to the $\bar{R}_n^0(p, \lambda_l)$. Various other forms for \bar{R}^0 have proved convenient under different circumstances.

(d) We calculate the quantities

$$\bar{y}_n^1(p, \lambda_l) = \int_0^\infty d(1-\omega_x)(1-\omega_x)^n \frac{\bar{R}^0(p, \omega_x, \lambda_l)}{\mu(\lambda_l) - p\omega_x}. \quad (10)$$

The upper limit of this integration is actually 2, but it can be taken as ∞ if the source is monodirectional and if $\lambda_l - \lambda_0 \ll 2$. This is a convenient, though unnecessary approximation.

(e) We insert the $\bar{y}_n^1(p, \lambda_l)$ into the bracketed terms of (8) and call the new approximation to the right sides so obtained $\bar{R}_n^1(p, \lambda_l)$.

Since this last step corresponds to step (b) we have a closed cycle defining an iteration procedure. This cycle of operations is repeated until it yields negligible change in the quantities $\bar{y}_n(p, \lambda_l)$. These values are then used in exactly this same way to calculate the $\bar{y}_n(p, \lambda_{l+1})$.

This iteration procedure can be used to calculate the $\bar{y}_n(p, \lambda_l)$. For this first interval it may be convenient to take $\bar{R}^0(p, \omega_x, \lambda_l) = D(p, \omega_x, \lambda_l)$ in the first iteration, since the low orders of scattering always predominate very close to the smallest wavelength for the problem.

As was mentioned in the third step of the iteration cycle, the main problem of this method of solution is that of determining a well-behaved function corresponding to r approximately known moments. The most widely used general procedure for solving such a moment problem is that of combining the moments into coefficients of some orthogonal polynomial system. (For a discussion of this, see reference 6.) This polynomial method is especially useful if a proper "weight function" can be ascertained from available information about the distribution. Experience indicated that our knowledge of R and the R_n is insufficient to make use of the polynomial method. We could devise no polynomial system which gave adequate convergence, and were forced to seek new methods for approximating functions.

The form of \bar{R}^0 given in (9) corresponds to a different method of using moments to approximate a distribution

function. This method, which proved very satisfactory, is described in Appendix B. It is a generalization of a type of numerical integration due to Gauss. (Szegő¹¹ and Chandrasekhar¹ give good discussions of this type of numerical integration.) Gauss' type of numerical integration may be regarded as a method for approximating some standard function by a sum of Dirac δ -functions. The generalization which we use substitutes continuous functions such as the exponentials of (9) for the δ -functions. This procedure is particularly accurate and flexible when integrals of a function are desired in terms of moments of the function. This is just what we need, since we must evaluate the integrals (10).

V. ACCURACY OF THE CALCULATIONS

Of the two types of approximations involved, the use of finite integration steps is less troublesome than the use of a finite number of moment equations. It is always possible to decrease the interval size or use a better integration procedure to obtain the desired accuracy. Since the y_n are all continuous functions of λ , no special difficulties arise. It is quite advantageous to make use of our *a priori* knowledge of the y_n to decrease the number of intervals or to increase the accuracy of the integration. Thus, near the singularity the y_n will change rapidly with λ and fine integration intervals should be used; whereas if p and λ are such that the singularity is far away in the (p, λ) plane, coarse integration intervals can be used. Also, in plane, monodirectional, monoenergetic problems the y_n behave as $(\lambda - \lambda_0)^n$ near λ_0 . The integration should be weighted to take advantage of this knowledge.

With regard to the use of a limited number of moment equations and therefore limited information about R , we may say several things:

(a) All of our present knowledge of photon directional distributions indicates that oscillations or sharp discontinuities which would require many moments for their description are not an essential feature of this problem. It is true that if the source is monodirectional and monoenergetic the first scattered beam is indeed a δ -function; the second scattered beam contains a step function discontinuity; and in general the n 'th order of scattering contains a discontinuity in the $(n-2)$ derivative.¹² However, these discontinuities are a feature of a particular source type, and they tend to wash out as the penetration increases.¹³

(b) Our feeling that a relatively small number of moment Eqs. (8) may suffice is strengthened by examination of the fourth step in the iteration procedure.

¹¹ G. Szegő, *Orthogonal Polynomials* (American Mathematical Society, Colloquium Publications, 1939), vol. 23.

¹² L. V. Spencer and Fannie Jenkins, *Phys. Rev.* **76**, 1885 (1949).

¹³ In practice, the first scattered beam may be calculated separately; and the step function discontinuity in the second scattered beam may be easily reduced to a harmless discontinuity in the derivative by subtracting out and calculating separately a rectangular directional distribution whose ordinate is the same as that of the second scattering discontinuity.

Since the $\bar{y}_n(p, \lambda_i)$ are to be obtained by evaluating integrals, they will tend to be insensitive to the fine features of $R(p, \omega_x, \lambda_i)$.

(c) These deep penetrations are a heretofore unsolved problem, and no independent results exist which can serve as a check. We can, however, consider a sequence of approximations using 1, 2, 3, ... equations and see how rapidly it converges.

(d) An estimate of the accuracy obtained by using r moment equations can be made by calculating the eigenvalues of simplified problems with the methods discussed here.¹⁴ These can be compared with the values given by standard eigenvalue procedures. This was done in a preliminary investigation. In the homogeneous Wick equations corresponding to constant and linear mean free paths we approximated R with Gaussians (i.e., $\bar{R} = \sum_m (\eta_m / \beta_m) \exp(-\frac{1}{2}\theta^2 / \beta_m)$). The surprising result was that as few as two moment equations yielded the eigenvalue at least as accurately as any of the eigenvalue methods of reference 4.

Because of this result, it seemed reasonable in mono-directional source problems to use only two moment equations and to approximate R by a single exponential of the form given by (9).

On the other hand, in plane isotropic source problems the angular distribution has a long and very strong tail. For these problems it was necessary to use four moment equations, in order to describe both the peak at $\omega_x = 1$ and the tail. Here the approximation was of the form

$$R = \frac{\eta_0}{\beta_0 + (1 - \omega_x)} + \frac{\eta_1}{\beta_1 + (1 - \omega_x)}. \quad (11)$$

(This analytic form is exact for the unscattered radiation.)

VI. THE "MEAN SQUARE DEFLECTION" PARAMETER

The parameter $g_1(p, \lambda) = y_1(p, \lambda) / y_0(p, \lambda)$ is a very useful quantity which has some physical significance. From the definition of the angular moments, we see that for small deflections θ , $g_1(p, \lambda) = \langle 1 - \omega_x \rangle_{\lambda} \cong \langle \theta^2 / 2 \rangle_{\lambda}$. Thus, the $g_1(p, \lambda)$ is essentially a mean square deflection and measures the angular "spread."

The $g_1(p, \lambda)$ has a number of very convenient properties. It is a smooth, positive, bounded, slowly varying function of p and λ . As mentioned in Sec. III, the g_1 can be regarded as playing the role of an eigenvalue. A knowledge of the $g_1(p, \lambda)$ makes it possible to reduce the system of Eqs. (4) to a single equation, similar to Eq. (3) of reference 3, for the flux $y_0(p, \lambda)$. If $y_1(p, \lambda)$ is expressed as $g_1(p, \lambda)y_0(p, \lambda)$, the first of Eqs. (4)

¹⁴ Such problems would be the homogeneous equations with constant or linear total cross section. These problems were first treated by Wick. See reference 4 and Appendix A.

($n=0$) becomes

$$\begin{aligned} & [\mu(\lambda) - p + pg_1(p, \lambda)]y_0(p, \lambda) \\ & = \int_0^\lambda d\lambda' k(\lambda, \lambda')y_0(p, \lambda') + \text{source}. \end{aligned}$$

The asymptotic solution of the equation, for $\mu \sim \mu_s$ is

$$\begin{aligned} & [\mu(\lambda) - p + pg_1(p, \lambda)]y_0(p, \lambda) \\ & = \exp \left[C \int^\lambda d\lambda' \frac{1}{\mu(\lambda') - p + pg_1(p, \lambda')} \right], \quad (12) \end{aligned}$$

where $C = k(\lambda, \lambda)$.^{3,15}

Equation (12) differs from Eq. (3) reference 3 by the additional term $pg_1y_0(p, \lambda)$. This term disappears if one assumes a "straight ahead" approximation, i.e., $g_1 = 0$, as in reference 3. The equation without the term $pg_1y_0(p, \lambda)$ also pertains to a somewhat different problem. If one regards the variable x in (1) as the total path length traveled, rather than as the distance attained from the source, then ω_x must be replaced by 1 in this equation and the coefficient g_1 never appears. Accordingly the factor pg_1 in (12) represents an additional absorption due to obliquity of path, which makes the depth of penetration shorter than the path length traveled.

VII. INVERSION OF THE FOURIER-LAPLACE TRANSFORM

In order to obtain the spectral density as a function of penetration away from the source, it is necessary to evaluate numerically the complex integral

$$Y_0(x, \lambda) = \frac{1}{2\pi i} \int_{-i\infty}^{i\infty} dp e^{-px} y_0(p, \lambda). \quad (13)$$

We have a number of pieces of information with which to work in making this inversion:

(a) We have values of \bar{y}_0 for four or five real values, p_i , of p . These numbers are approximations, as discussed earlier.

(b) $y_0(p, \lambda)$ is a smooth function of p and $Y_0(x, \lambda)$ is a smooth function of x . The values p_i will have been chosen conveniently for interpolation.

(c) Both y_0 and Y_0 are positive functions.

(d) $\exp(-px)y_0(p, \lambda)$ has a saddle point on the real axis as discussed earlier.

(e) We know approximately the variation of both y and Y for small p and small x .

(f) All singularities of $y_0(p, \lambda)$ are located on the real axis, as discussed earlier.

(g) We know the type as well as the location of the singularities of $y_0(p, \lambda)$ and the corresponding asymptotic form of $Y_0(x, \lambda)$.

¹⁵ The eigenvalue \bar{C} mentioned in Appendix A is related to g_1 by

$$\bar{C} = C / [1 + pg_1 / (\mu - p)].$$

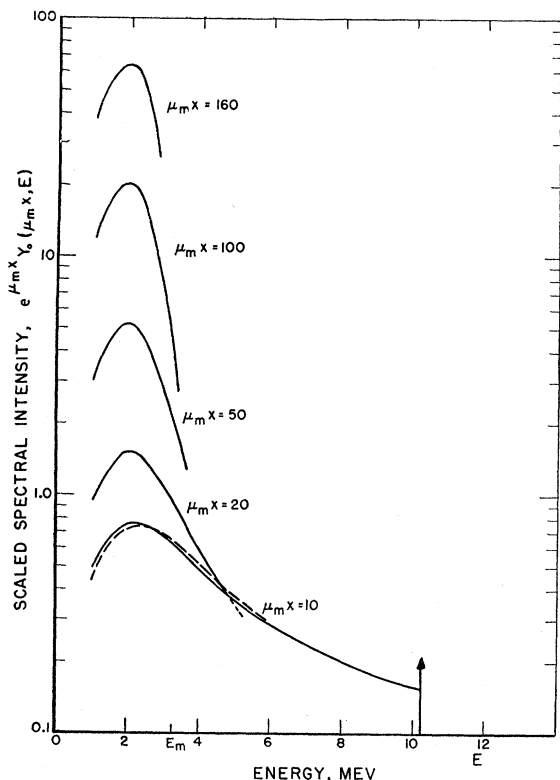


FIG. 1. Scaled differential x-ray intensity in units (Mev/cm²sec)/Mev at various distances x from a plane monodirectional source of 10.22-Mev photons in Pb. The factor $\exp(-\mu_m x)$ has been divided out. The strength of the source is 10.22 Mev/cm² sec. The narrow beam attenuation coefficient of the source radiation is 0.561 cm⁻¹, while that of the most penetrating component is 0.466 cm⁻¹.

The method of inversion which first suggests itself is saddle point integration, because of (d) and (f). In order to do such an integration, we would fit an approximate curve or curves to the points $\bar{y}_0(p, \lambda)$, determine the function and a few derivatives at the saddle point, and substitute in the proper formula. In so doing we would be taking no advantage of important information [e.g., item (g)] which we might have about higher derivatives of y_0 .

In general, we can expect that most accurate results can be obtained by an inversion process which incorporates a maximum of the available information. The inversion technique which we actually used is described in Appendix C. Basically it consisted of fitting the values with smooth, positive functions which have both the correct type of singularity and the correct behavior for small p . These functions were then inverted exactly. The results were considered reliable for that range of x where the saddle point method could have been used.

VIII. NUMERICAL APPLICATIONS

In order to explore the range of application of these methods, we made calculations for both a monotonic attenuation coefficient and an attenuation coefficient

which has a minimum within the range of integration. We also made calculations for both plane monodirectional and plane isotropic source types. The attenuation coefficients were furnished by White,¹⁶ and the full Klein-Nishina differential scattering cross section was used.

The calculations were not extended to include components below 1 Mev in energy. Also, the isotropic source calculation was limited to a single value of p . Economy of effort was the main reason for these limitations. If desired, low energies (which come quickly into relative equilibrium) and small values of p can perhaps be more easily calculated by the polynomial method.⁶

A. Plane Monodirectional 10.22-Mev Source in Pb

In this problem, $y_0(p, \lambda)$ was calculated for $p/\mu_m = 0, 0.65, 0.85, 0.95,$ and 0.98 . The Fourier-Laplace transform was inverted as in Appendix C. Figure 1 presents the resulting spectra, for penetrations up to $\mu_m x = 160$.¹⁷ The dashed line gives for comparison the results of a polynomial calculation for $\mu_m x = 10$. The same attenuation coefficients were used for both calculations. The agreement is within about 3 percent.

Notice that the ordinate is $\exp(+\mu_m x)Y_0(\mu_m x, E)$ rather than the exponentially decreasing $Y_0(\mu_m x, E)$. (If Y_0 had been plotted, it would have been necessary to use 70-cycle log paper!)

The main characteristics of the x-ray spectra of Fig. 1 are as follows: There is a δ -function source at 10.22 Mev, represented by the arrow. At 10.22 Mev there is a singly scattered component which varies as $\mu_0 x \exp(-\mu_0 x)$. Since we have discounted an exponential, this component behaves, in Fig. 1, as $\mu_m x \exp[-(\mu_0 - \mu_m)x]$. In general the components with energies above E_m (E_m corresponds to the minimum attenuation coefficient) behave asymptotically as $(\mu_m x)^{-\bar{c}/\bar{\mu}(\lambda)} \exp[-(\mu - \mu_m)x]$.¹⁸ As the energy approaches E_m from above, the exponential factor becomes weaker and $(\bar{C}/\bar{\mu})$ becomes larger. At E_m , the exponential factor becomes unity and the build-up is maintained asymptotically at approximately the rate $x^{-5/6} \exp(\frac{1}{2}\bar{b}x^{1/3})$.¹⁸

At low energies a relative equilibrium is established. (This means that at low energies the spectrum does not change shape as the penetration increases.) All components "build up" together over the exponential at approximately the rate $x^{-5/6} \exp(\bar{b}x^{1/3})$.¹⁸ The more penetrating the scattered component, the greater the

¹⁶ G. R. White, Natl. Bur. Standards Rep. 1003, 1952 (unpublished).

¹⁷ At high energies and great penetrations, the spectrum is not given. This is because the singularity for $\lambda < \lambda_m$ is located at $p = \mu(\lambda) > \mu_m$. Since we did no calculations for $p > 0.98\mu_m$ we did not, in general, approach very closely to the singularity for $\lambda < \lambda_m$. Thus, the saddle point for deep penetrations at these high energies lay outside the range of our calculations.

¹⁸ Refer to Appendix A for a summary of asymptotic penetration laws.

penetration at which this relative equilibrium is established.

Since the low energy components "build up" as $x^{-5/6} \exp(\bar{b}x^{1/3})$, whereas the E_m component "builds up" as $x^{-5/6} \exp(\frac{1}{2}\bar{b}x^{1/3})$, there must be an energy region in which a transition occurs from one asymptotic penetration law to the other. This nonequilibrium region becomes narrower with increasing penetration, and the difference between the penetration laws becomes more serious. Thus the spectrum becomes enormously steep at energies near E_m .

Perhaps the most striking feature of the spectra is a maximum at an energy substantially below $E_m \approx 3$ Mev. This maximum is apparently a feature of the equilibrium spectrum.¹⁹ It is located about at the energy at which the sum of the photoelectric and pair creation cross sections is a minimum. Whereas the steeply rising portion of the curve is determined by the minimum in the total cross section, the maximum may be determined by the interplay of photoelectric absorption and pair creation.

The $\bar{g}_1(\bar{p}, \lambda)$ given by these calculations is presented in Fig. 2. The linear rise near $\lambda_0 = 0.05$ represents first scattering. The dip at $\lambda \sim 0.2$ illustrates the fact that the components controlling the deep penetration have directional distributions strongly peaked at $(1 - \omega_x) = 0$.

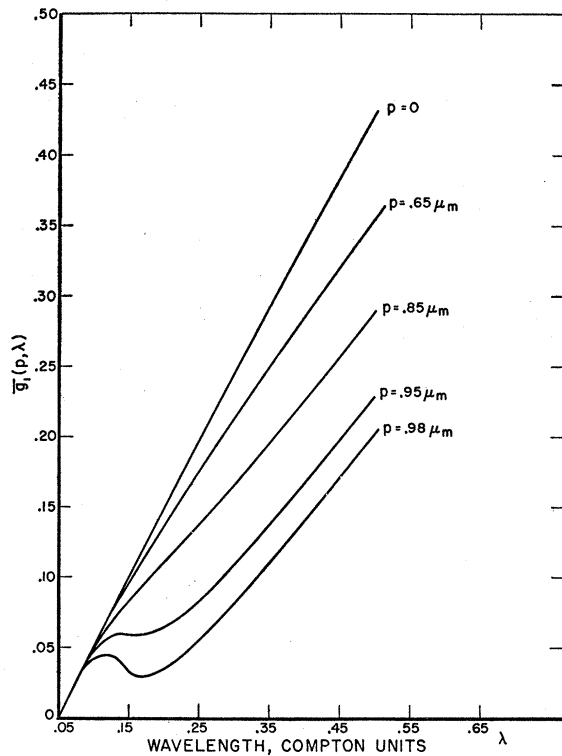


Fig. 2. The "mean square deflection" parameter $\bar{g}_1(\bar{p}, \lambda)$ for the Pb calculation.

¹⁹ In water there is a maximum in the equilibrium spectrum at about 70 keV which is determined by the interplay of scattering and photoelectric absorption. (See references 5 and 6.)

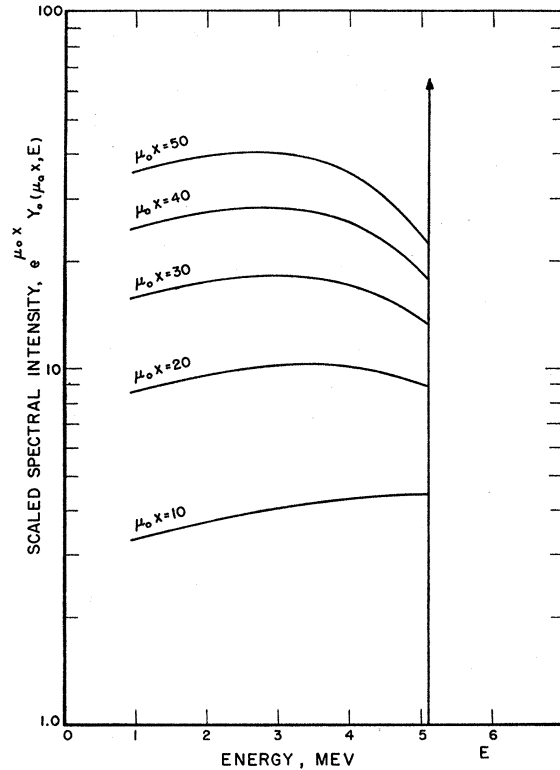


Fig. 3. Scaled differential x-ray intensity in units (Mev/cm²sec)/Mev at various distances x from a plane monodirectional source of 5.11-Mev photons in Fe. The factor $\exp(-\mu_0 x)$ has been divided out. The source strength is 5.11 Mev/cm² sec and the attenuation coefficient of the source radiation is 0.246 cm⁻¹.

Finally, at large λ the curves for different \bar{p} have nearly the same shape, indicating relative equilibrium in the directional distributions, as well as the flux, of the low energy components.

B. Plane Monodirectional 5.11-Mev Source in Fe

Calculations of $\bar{g}_0(\bar{p}, \lambda)$ were made at the values $\bar{p}/\mu_0 = 0, 0.65, 0.85,$ and 0.95 . Figure 3 presents the calculated spectral intensities for various penetrations.

The ordinate is $\exp(\mu_0 x) Y_0(\mu_0 x, E)$ rather than $Y_0(\mu_0 x, E)$. Since μ_0 is the smallest attenuation coefficient, all scattered components increase in Fig. 3. The lowest energy components reach relative equilibrium at relatively small penetrations. These equilibrium components "build up" at the rate $(\mu_0 x)^{\bar{C}/\mu_0}$, $\bar{C}/\mu_0 > 1$. Just below the source energy E_0 is a nonequilibrium region of the spectrum which narrows as the penetration increases. Since the trend of the build-up changes from x to $x^{\bar{C}/\mu_0}$ in this nonequilibrium region, the spectrum becomes increasingly steep.

The solid curves in Fig. 4 give the $\bar{g}_1(\bar{p}, \lambda)$ for this problem. They behave like $(\lambda - \lambda_0)$ near λ_0 , indicating single scattering. For large λ and for \bar{p} near μ_0 , the curves tend to become parallel, indicating an approach

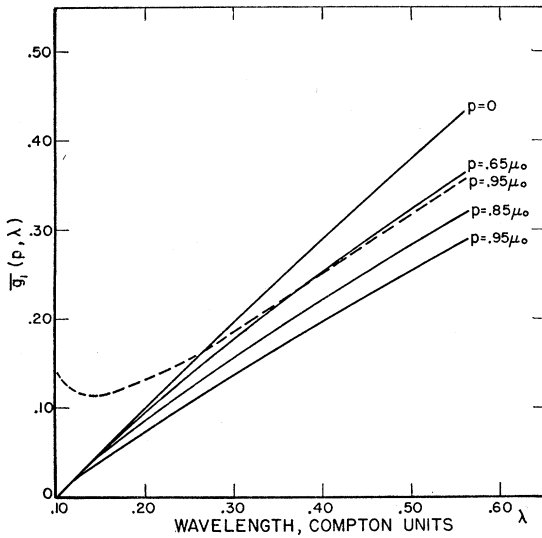


FIG. 4. The parameter $\bar{g}_1(p, \lambda)$ for the plane monodirectional Fe calculation (solid curves) and the plane isotropic Fe calculation (dashed curve).

to relative equilibrium in the directional distributions of the low energy components.²⁰

C. Plane Isotropic 5.11-Mev Source in Fe

This calculation was made only for the value $p/\mu_0 = 0.95$. The dashed line in Fig. 4 gives the resulting \bar{g}_1 . Notice that it starts at a finite value corresponding to once scattered radiation. It then dips, indicating a concentration of scattered radiation with directions near $\theta=0$. Finally, it tends to become parallel with the solid curves, indicating the establishment of equilibrium.

In this isotropic problem, four moment equations were used, whereas only two were used in the corresponding monodirectional problem. This gives rise to a slight difference in the slope of the \bar{g}_1 in the equilibrium region of wavelengths. (The comparison is between the two curves with $p/\mu_0=0.95$.) The effect of this on the asymptotic penetration law is to change the exponent of the build-up factor by perhaps two or three percent.

IX. REMARKS

In conclusion it may be worth noting that the work required to accomplish a second calculation like the Pb calculation of Fig. 1 would be of the order of three or four man weeks.

As mentioned in the first footnote, pair production has been considered as being simply a mechanism for absorption. Cascade processes have been neglected. One may wonder at what source energy (for a given

²⁰ Since the attenuation coefficient is nearly linear, the slope $\dot{g}_1 = \partial \bar{g}_1 / \partial \lambda$ for the equilibrium portions of the curves is related to Wick's eigenvalue in the following way:

$$\bar{C} = C / (1 + p \dot{g}_1 / \dot{\mu}).$$

(See footnotes 14 and 15 and Appendix A.)

material) cascade processes become sufficiently important to make this a poor approximation. Some work has been done on this problem by Cohen and Plesset,²¹ who attempt a rough calculation of the effect in Pb and U. It is our intention to concentrate some effort on this and related problems in the future.

In this paper we have concentrated on great penetrations. These methods of calculation can probably also be used effectively to study the spectral distributions of those x-rays which reverse their direction and penetrate back to and behind the source.

The writer wishes to thank Dr. U. Fano for many discussions and suggestions, and to acknowledge the able assistance of Mrs. Fannie Stinson, who did most of the numerical work for this paper.

APPENDIX A. SUMMARY OF CALCULATIONS OF ASYMPTOTIC PENETRATION LAWS

(a) The initial work on this problem followed the "straight ahead" approximation method, i.e., it disregarded the small deflections which accompany Compton scattering with small changes of wavelength. In addition to this, reference 2 assumed, in particular, that the total ("narrow beam") attenuation coefficient $\mu(\lambda)$ increases steadily as the photon wavelength increases in the course of successive Compton scatterings. Under these assumptions the spectral energy density $Y(x, \lambda)$ was shown to vary asymptotically as

$$Y(x, \lambda) \propto x^{C/\dot{\mu}_0} e^{-\mu_0 x}, \quad (1)$$

where $C = k(\lambda, \lambda)$ is the probability density for Compton scattering without wavelength change and $\mu_0, \dot{\mu}_0$ are the zero'th and first derivatives with respect to λ of the attenuation coefficient μ at the smallest source wavelength.

(b) Reference 3 removed the restriction of a monotonically increasing attenuation coefficient and treated the case of an attenuation coefficient which has a minimum value $\mu_m = \mu(\lambda_m)$ at some wavelength greater than the smallest source wavelength λ_0 . The asymptotic penetration law for those spectral components with wavelengths greater than λ_m was found to be

$$Y(x, \lambda) \propto [x^{-5/6} \exp(bx^{1/3})] e^{-\mu_m x}, \quad (2)$$

where $b = 3[\pi^2 C^2 / 2 \ddot{\mu}_m]^{1/3}$, and $\ddot{\mu}_m = (d^2 \mu / d\lambda^2)_m$. Surprisingly, the λ_m component was found to vary asymptotically as

$$Y(x, \lambda_m) \propto [x^{-5/6} \exp(\frac{1}{2} b x^{1/3})] e^{-\mu_m x}. \quad (3)$$

(c) The small angular deflections have a substantial influence on the intensity at deep penetrations. These deflections were taken into account in reference 4, but only for a $\mu(\lambda)$ which increases monotonically with increasing λ . The resulting asymptotic behavior was found to be

$$Y(x, \omega_x, \lambda) \propto x^{\bar{C}/\dot{\mu}_0} e^{-\mu_0 x}, \quad (4)$$

²¹ S. T. Cohen and E. H. Plesset, Rand Corporation Report RAD-264, May 20, 1948 (unpublished).

where $(-\bar{C})$ is the lowest eigenvalue of a certain Schrödinger type equation. The resemblance to (1) is apparent, and indeed C is an upper limiting value to \bar{C} . This progress represents an application of a method used by Wick²² in solving the analogous problem of neutron penetration.

(d) The case of a constant attenuation coefficient has importance even though it is physically nonexistent. Application of the methods of references 2 and 3 is straightforward in the "straight ahead" approximation, and the result is

$$Y(x, \lambda) \propto \exp[2(C(\lambda - \lambda_0)x)^{\frac{1}{2}}]e^{-\mu_0 x}. \quad (5)$$

Angular deflections can be taken into account by the method of Wick, which yields the asymptotic form

$$Y(x, \omega_x, \lambda) \propto \exp[2(\bar{C}(\lambda - \lambda_0)x)^{\frac{1}{2}}]e^{-\mu_0 x}, \quad (6)$$

where $(-\bar{C})$ is again the lowest eigenvalue of a Schrödinger type equation.

(e) The situation in which the attenuation coefficient decreases monotonically has never been discussed even though it is pertinent if $\lambda < \lambda_m$. The asymptotic penetration law in straight ahead approximation is

$$Y(x, \lambda) \propto x^{-C/\bar{\mu}(\lambda)}e^{-\mu(\lambda)x}. \quad (7)$$

Angular deflections change this to

$$Y(x, \omega_x, \lambda) \propto x^{-\bar{C}/\bar{\mu}(\lambda)}e^{-\mu(\lambda)x}, \quad (8)$$

where $(-\bar{C})$ is the lowest eigenvalue of a Schrödinger type equation very similar to that associated with expression (4).

(f) To complete the picture, we must discuss (b) generalized to include angular deflections. A study of this problem has been made by Fano.^{22a} The asymptotic penetration law behaves like

$$Y(x, \omega_x, \lambda) \propto [x^{-5/6} \exp(\bar{b}x^{1/3})]e^{-\mu_m x}, \quad (9)$$

where $\lambda > \lambda_m$. The λ_m component obeys the asymptotic law

$$Y(x, \omega_x, \lambda_m) \propto [x^{-5/6} \exp(\frac{1}{2}\bar{b}x^{1/3})]e^{-\mu_m x}, \quad (10)$$

where $\bar{b} = b(\bar{C})$, b has the meaning previously ascribed in paragraph (b), and \bar{C} is the eigenvalue of a constant mean free path problem obtained by completely ignoring variations of μ near μ_m .

(g) Associated with each asymptotic penetration law is a singularity in the spatial Fourier-Laplace transform variable $y(p, \omega_x, \lambda)$. The following is a list of these singularities:

$$y(p, \omega_x, \lambda) \propto \left[\frac{1}{\mu_0 - p} \right]^{\xi} \quad (\text{monotonically increasing } \mu(\lambda)),$$

$$y(p, \omega_x, \lambda) \propto \left[\frac{1}{\mu(\lambda) - p} \right]^{\xi(\lambda)} \quad (\text{monotonically decreasing } \mu(\lambda)),$$

$$y(p, \omega_x, \lambda) \propto \{ \exp[(\lambda - \lambda_0)/(\mu_0 - p)] \}^{\xi} \quad (\text{constant } \mu, \mu = \mu_0),$$

$$y(p, \omega_x, \lambda) \propto [\exp(\mu_m - p)^{-\frac{1}{2}}]^{\xi} \quad (\mu(\lambda) \text{ with minimum at } \lambda_m).$$

The parameter ξ must be determined, in every case, by determining the lowest eigenvalue of a Schrödinger type equation.

APPENDIX B. A METHOD FOR APPROXIMATING A FUNCTION FROM A KNOWLEDGE OF ITS MOMENTS

We want to approximate a distribution function $H(x)$ by a sum of terms

$$H(x) \approx \eta_1 f(x, \beta_1) + \eta_2 f(x, \beta_2) + \eta_3 f(x, \beta_3) + \dots + \eta_n f(x, \beta_n), \quad (1)$$

where the η_i and β_i are parameters to be fitted so that the first $2n$ moments of the approximate function agree with the corresponding moments of $H(x)$. (Notice that in contrast to the polynomial method, each term on the right involves two constants to be determined instead of one, and that all the terms have the same form.) This can be accomplished for a broad class of functions $f(x, \beta_i)$.

1. The Gauss Method of Numerical Integration

According to this well-known integration technique, if an integral

$$\int_c^d H(x)S(x)dx \quad (2)$$

is to be evaluated, $H(x)$ and all its moments over the interval being known, the most accurate n point numerical integration that can be performed is to take

$$\int_c^d H(x)S(x)dx \approx \sum_{i=1}^n \eta_i S(\beta_i), \quad (3)$$

where the β_i are the zeros of a polynomial $h_n(x)$, which is the n 'th self-adjoint polynomial associated with the weight function $H(x)$. The η_i are the so-called Christoffel numbers, which may be calculated from the formula

$$\left(\frac{dh_n}{dx} \right)_{\beta_i} \eta_i = \int_c^d \frac{H(x)h_n(x)}{x - \beta_i} dx. \quad (4)$$

(In Gauss' original scheme, $H(x) = 1$, $c = -1$, $d = 1$.)

The reason for the accuracy of this approximation is that in this procedure we are actually replacing $H(x)$ by

²² G. C. Wick, Phys. Rev. **75**, 738 (1949).

^{22a} This material is part of a comprehensive report on the subject to be published in the J. Research Natl. Bur. Standards.

a much more manageable function, namely,

$$H(x) \approx \sum_{i=1}^n \eta_i \delta(x - \beta_i). \tag{5}$$

The scheme for choosing the β_i, η_i is such that the first $2n$ moments of the sum of Dirac delta-functions are made to agree with the first $2n$ moments of $H(x)$.

From our standpoint the most remarkable feature about this method of describing $H(x)$ is the fact that the β_i and η_i are all determined from a knowledge of the moments of $H(x)$, rather than from the function itself. Thus the δ -function is one of the functions which can be used in the approximation (1).

2. Generalization to Other Types of Functions

If we multiply (5) by x^m and integrate over x , we obtain the following set of equations, where $H_m = \int_c^d x^m H(x) dx$:

$$\begin{aligned} \eta_1 &+ \eta_2 &+ \dots + \eta_n &= H_0 \\ \eta_1 \beta_1 &+ \eta_2 \beta_2 &+ \dots + \eta_n \beta_n &= H_1 \\ \eta_1 \beta_1^2 &+ \eta_2 \beta_2^2 &+ \dots + \eta_n \beta_n^2 &= H_2 \\ &\vdots &&\vdots \\ &\vdots &&\vdots \\ \eta_1 \beta_1^{2n-1} &+ \eta_2 \beta_2^{2n-1} &+ \dots + \eta_n \beta_n^{2n-1} &= H_{2n-1}. \end{aligned} \tag{6}$$

These are $2n$ equations in $2n$ unknowns. The equations are nonlinear in half of the unknowns.

Since the first n self-adjoint polynomials can be obtained from a knowledge of the first $2n$ moments of the weight function, the polynomial $h_n(x)$ is determined by the known constants H_m . The zeros of $h_n(x)$ and the relations (4) determine the β_i and η_i which satisfy this nonlinear system of equations.

A set of equations with exactly the same form as (6) can be shown to obtain if we take moments of the relation (1), where $f(x, \beta_i)$ may be one of the following group of functions:

- (a) $f(x/\beta_i), c \leq x/\beta_i \leq d$, where $f(x/\beta_i)$ is any function, and c, d are arbitrary constants such that moments of $f(x/\beta_i)$ over this range exist.
- (b) $x^{\beta_i} e^{-x}, 0 \leq x \leq \infty$.
- (c) $e^{-x} {}_1F_1(-\beta_i; 1; -x), 0 \leq x \leq \infty$, where ${}_1F_1$ is the confluent hypergeometric function.
- (d) $x^{\beta_i} (1-x)^{A-\beta_i}, 0 \leq x \leq 1, A$ arbitrary.

3. Illustration

As a very simple illustration, suppose we have four moments H_m of a function $H(x), 0 \leq x \leq \infty$, and we want to approximate $H(x)$ by two exponentials. We write

$$H(x) \approx \frac{\eta_1}{\beta_1} e^{-x/\beta_1} + \frac{\eta_2}{\beta_2} e^{-x/\beta_2}.$$

Taking moments, we have the relations (6) for this

simple problem:

$$\begin{aligned} \eta_1 + \eta_2 &= H_0/0! = H_0^*, \\ \eta_1 \beta_1 + \eta_2 \beta_2 &= H_1/1! = H_1^*, \\ \eta_1 \beta_1^2 + \eta_2 \beta_2^2 &= H_2/2! = H_2^*, \\ \eta_1 \beta_1^3 + \eta_2 \beta_2^3 &= H_3/3! = H_3^*. \end{aligned}$$

Using "orthogonality relations" we obtain the polynomial which is "self-adjoint" with respect to the "weight function" whose "moments" are the H_m^* :

$$h_2^*(x) = x^2 - ax + b,$$

where

$$a = \frac{H_3^* H_0^* - H_2^* H_1^*}{H_2^* H_0^* - H_1^{*2}}; \quad b = \frac{H_3^* H_1^* - H_2^{*2}}{H_2^* H_0^* - H_1^{*2}}.$$

The roots of the equation $h_2^*(x) = 0$ are

$$\beta_1 = \frac{1}{2} [a - (a^2 - 4b)^{\frac{1}{2}}]; \quad \beta_2 = \frac{1}{2} [a + (a^2 - 4b)^{\frac{1}{2}}].$$

For the corresponding "Christoffel" numbers, we have

$$\begin{aligned} \eta_1 &= \frac{1}{2\beta_1 - a} \int_0^\infty (x - \beta_2) H_0^*(x) dx = \frac{\beta_2 H_0^* - H_1^*}{(a^2 - 4b)^{\frac{1}{2}}}; \\ \eta_2 &= \frac{1}{2\beta_2 - a} \int_0^\infty (x - \beta_1) H_0^*(x) dx = \frac{\beta_1 H_0^* - H_1^*}{(a^2 - 4b)^{\frac{1}{2}}} = H_0^* - \eta_1. \end{aligned}$$

APPENDIX C. INVERSION OF THE FOURIER-LAPLACE TRANSFORM

1. Approximating a Function if Several Values of the Function are Known

If we have several values $H_m = H(x_m)$ of a function $H(x)$, we may make the same type of approximation as in Appendix B, provided the H_m are properly spaced. The useful function types in general differ from those of Appendix B. (This method has been worked out independently and applied to a similar problem by a UCLA group.)²³

As an example, suppose we choose four values H_0, H_1, H_2, H_3 of a function which we want to approximate by exponentials. The approximate function must agree with the exact one at the values (H_m, x_m) . The x_m are so chosen that $(x_{m+1} - x_m) = (x_m - x_{m-1})$. We write

$$H(x) \approx \eta_0 e^{-\beta_0 x} + \eta_1 e^{-\beta_1 x}.$$

Next, we define $\beta_0^* = e^{-\beta_0(x_1 - x_0)}$; $\beta_1^* = e^{-\beta_1(x_1 - x_0)}$; $\eta_0^* = \eta_0 e^{-\beta_0 x_0}$; $\eta_1^* = \eta_1 e^{-\beta_1 x_0}$. The set of equations which must be solved to pass the approximate function through the values (H_m, x_m) is thereby reduced to the form (6) of Appendix B.

A class of functions most useful in making this type of approximation is the class $[W(x)]^\beta$, where $W(x)$ is any function and β is a constant. All the singularities which may determine the asymptotic form of $Y_0(x, \lambda)$ are of this type.

²³ Greenfield, Specht, Kratz, and Hand, J. Opt. Soc. Am. 42, 6 (1952).

2. Numerical Applications

In order to make the best possible use of our information about $y_0(p, \lambda)$ we accomplish the inversion in the following ways:

(a) Where the controlling singularity has the form $(\mu_0 - p)^{-\beta}$, as in the problem of a monodirectional source in Fe, we made the approximation

$$y_0(p, \lambda) \approx e^{-dp} [\eta_1(\mu_0 - p)^{-\beta_1} + \eta_2(\mu_0 - p)^{-\beta_2}].$$

Here, d is an arbitrary constant which is chosen to make the approximate function as smooth as possible. We chose this method of introducing such a smoothness parameter because it does not make the exact inversion more difficult or complicated. The inverted function $Y_0(x, \lambda)$ is then given by the relation

$$Y_0(x, \lambda) \approx e^{-\mu_0(x+d)} \left[\frac{\eta_1}{\Gamma(\beta_1)} (x+d)^{\beta_1-1} + \frac{\eta_2}{\Gamma(\beta_2)} (x+d)^{\beta_2-1} \right].$$

Notice that the d merely introduces a shift in the penetration.

(b) In the problem of a monodirectional source in Pb, for $\lambda < \lambda_m$, where the controlling singularity has the form $(\mu - p)^{-\beta(\lambda)}$, we made the approximation

$$(\mu_0 - p)^2 y_0(p, \lambda) \approx e^{-dp} [\eta_1(\mu - p)^{-\beta_1} + \eta_2(\mu - p)^{-\beta_2}].$$

Here, d is again chosen for smoothness. Notice the factor $(\mu_0 - p)^2$ on the left. This discounts features of y_0 which are characteristic of the source and which tend to obscure the approach to asymptoticity. (The unscattered component of the radiation is not included in y_0 .) Taking this factor into account explicitly in this way gives greater accuracy by introducing one more piece of our information. When this approximation is inverted, the flux is given by the expression

$$Y_0(x, \lambda) \approx e^{-\mu(x+d)} \sum_{i=1,2} \frac{\eta_i}{\Gamma(\beta_i+2)} (x+d)^{\beta_i+1} \times {}_1F_1[2; 2+\beta_i; -(\mu_0 - \mu)(x+d)].$$

(c) Finally, in the problem of a monodirectional source in Pb, for $\lambda > \lambda_m$, where the singularity has the form $[\exp(\mu_m - p)^{-\frac{1}{2}}]^\beta$, we use the approximation

$$(\mu_0 - p)^2 y_0(p, \lambda) \approx e^{-dp} \{ \eta_1 \exp[\beta_1/(\mu_m - p)^{\frac{1}{2}}] + \eta_2 \exp[\beta_2/(\mu_m - p)^{\frac{1}{2}}] \},$$

with d again chosen for smoothness. The behavior of $y_0(p, \lambda)$ for small p is again taken into account explicitly.

In order to obtain the flux in this last case, we must find the inverse transform of the function $(\mu_0 - p)^{-2} \exp[\beta_i/(\mu_m - p)^{\frac{1}{2}}]$. There are various ways in which this inversion can be accomplished, but the one which turned out to be most convenient was to expand the exponential and invert term by term. This yields a strongly converging sum:

$$\begin{aligned} & \frac{1}{2\pi i} \int_{-i\infty}^{i\infty} dpe^{-p(x+d)} (\mu_0 - p)^{-2} \exp[\beta_i/(\mu_m - p)^{\frac{1}{2}}] \\ &= e^{-\mu_m(x+d)} \sum_{n=0}^{\infty} \frac{\beta_i^n (x+d)^{\frac{1}{2}n+1}}{n!(\frac{1}{2}n+1)!} \\ & \times {}_1F_1[2; \frac{1}{2}n+2; -(\mu_0 - \mu_m)(x+d)]. \end{aligned}$$

Some idea of the convergence can be gained from the fact that in the Pb problem it took about 15 terms to give an accurate answer for a penetration of 180 mean free paths. This is not so much work as it seems, because the alternate terms of the sum can be readily derived from each other. Using the formulas connecting the various ${}_1F_1$'s we made tabulations and graphs of the first 16 of these functions.

This expansion into a sum of ${}_1F_1$'s has physical significance. Since the constant β in the exponent contains, asymptotically, the factor $k(\lambda, \lambda) = C$,³ this is actually a sort of expansion in orders of scattering. Thus, the fact that 15 terms suffice at 180 mean free paths means that as few as 15 orders of scattering are important at this penetration!